High resolution photoelectron imaging of UO− and UO2 − and the low-lying electronic states and vibrational frequencies of UO and UO2

Joseph Czekner, Gary V. Lopez, and Lai-Sheng Wang

Citation: The Journal of Chemical Physics **141**, 244302 (2014); doi: 10.1063/1.4904269
View online: http://dx.doi.org/10.1063/1.4904269
View Table of Contents: http://scitation.aip.org/content/aip/journal/jcp/141/24?ver=pdfcov
Published by the AIP Publishing

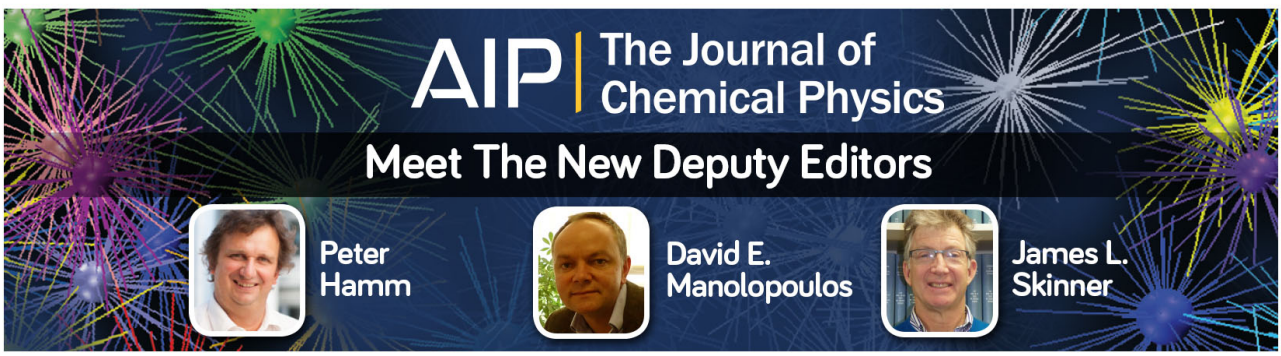

High resolution photoelectron imaging of UO^- and UO_2^- and the low-lying electronic states and vibrational frequencies of UO and UO_2

Joseph Czekner, Gary V. Lopez, and Lai-Sheng Wang[a)]
Department of Chemistry, Brown University, Providence, Rhode Island 02912, USA

(Received 13 October 2014; accepted 3 December 2014; published online 22 December 2014)

We report a study of the electronic and vibrational structures of the gaseous uranium monoxide and dioxide molecules using high-resolution photoelectron imaging. Vibrationally resolved photoelectron spectra are obtained for both UO^- and UO_2^-. The spectra for UO_2^- are consistent with, but much better resolved than a recent study using a magnetic-bottle photoelectron analyzer [W. L. Li *et al.*, J. Chem. Phys. **140**, 094306 (2014)]. The electron affinity (EA) of UO is reported for the first time as 1.1407(7) eV, whereas a much more accurate EA is obtained for UO_2 as 1.1688(6) eV. The symmetric stretching modes for the neutral and anionic ground states, and two neutral excited states for UO_2 are observed, as well as the bending mode for the neutral ground state. These vibrational frequencies are consistent with previous experimental and theoretical results. The stretching vibrational modes for the ground state and one excited state are observed for UO. The current results for UO and UO_2 are compared with previous theoretical calculations including relativistic effects and spin-orbit coupling. The accurate experimental data reported here provide more stringent tests for future theoretical methods for actinide-containing species. © *2014 AIP Publishing LLC*. [http://dx.doi.org/10.1063/1.4904269]

I. INTRODUCTION

The uranium monoxide and dioxide molecules have been the focus of many recent theoretical investigations because of their complex bonding and electronic structure due to strong relativistic effects, spin-orbit coupling, and strong electron correlation effects.[1–8] These factors make even the simplest actinide-containing molecules quite challenging electronic systems computationally. In order to calibrate the accuracy of various calculations, highly accurate experimental data are needed. High-resolution photoelectron imaging of anions is a powerful experimental technique to obtain highly accurate electronic and vibrational information for the corresponding neutral molecules.[9]

Earlier experimental work on uranium oxides concerned their infrared spectra recorded in argon and krypton matrices.[10–12] These experiments suggested the ground state of UO_2 to be $^3H_{4g}$. However, experiments in a neon matrix suggested that the vibrational frequencies matched better with a ground state of $^3\Phi_{2u}$.[1] Subsequently, it was shown that uranium has significant interactions with the argon matrix, leading to the so-called "ground state reversal," because argon is four times more polarizable than neon.[13,14] However, this matrix effect was not observed in fluorescence spectroscopy experiments.[15] Further, gas phase experimental and theoretical studies confirmed the $^3\Phi_{2u}$ ground state with an electron configuration of $(7s\sigma_g)^1(5f\phi_u)^1$.[1,4,16–19] Recently, the Wang group reported a photoelectron spectroscopy (PES) study of UO_2^- using a magnetic-bottle PE analyzer and a broad photon energy range.[20] Significant electron correlation effects were observed, as manifested by numerous two-electron transitions. The experimental data were interpreted by high-level theoretical calculations, which also confirmed the ground state of UO_2^- as $^2\Phi_{5/2u}$ $[(7s\sigma_g)^2(5f\phi_u)^1]$ and that of UO_2 as $^3\Phi_{2u}$ $[(7s\sigma_g)^1(5f\phi_u)^1]$.

There have also been numerous experimental and theoretical works pertaining to UO. Similar to UO_2, infrared spectroscopy on UO was carried out in argon and krypton matrices in early experimental works, reporting a vibrational frequency of ~820 cm^{-1}.[10,12] Later experiments in a neon matrix found this frequency to be 889.5 cm^{-1}.[1] Gas phase investigations on UO $X(\Omega = 4)$ reported the first vibrational interval for the ground state of UO to be $\Delta G_{1/2} = 882.35$ cm^{-1}, which was found to be perturbed in the $v'' = 0–4$ range.[21] A deperturbation analysis was performed to derive a diabatic vibrational constant of 846.5 ± 0.6 cm^{-1}.[21] Two recent theoretical studies predicted the unperturbed vibrational frequency to be 846 and 869.12 cm^{-1}.[1,8] To the best of our knowledge, the large matrix shifts on the UO vibrational frequency have not been investigated theoretically. Gas-phase fluorescence spectroscopy was used to determine the symmetries and angular momenta of the ground and many excited states of UO.[21–24] Ligand field theory calculations were carried out subsequently to determine the electron configurations of many of the experimentally observed states.[21] These calculations were used in further experimental works to determine the electric dipole moments and magnetic g factors for UO.[25] A recent study has been performed on the isoelectronic species of UF and UF^+, which show many similarities in the electronic structure.[26,27]

In the current article, we report a high resolution PE imaging study of UO^- and UO_2^-. In addition to providing

a)E-mail: lai-sheng_wang@brown.edu

accurate electron affinities (EAs) for UO and UO_2, low-lying electronic states and their vibrational frequencies have been obtained. Stretching frequencies for the ground state and one excited state of UO are reported. For UO_2, the symmetric stretching modes for the ground state and two excited states are obtained, as well as the bending mode of the ground state. Vibrational hot bands observed in the UO_2^- spectra have also allowed the frequency of the symmetric stretching mode for the UO_2^- anion to be measured. Two-electron transitions due to strong electron correlation effects are observed in the PE spectra of UO_2^-.

II. EXPERIMENTAL METHOD

The high resolution imaging apparatus has been described in detail recently,[28–31] and only a brief summary is provided here. The UO^- and UO_2^- anions were produced using a laser vaporization supersonic cluster source using an uranium disc target (Goodfellow Corporation). A pure helium carrier gas seeded with 10% Ar was used as the carrier gas. Oxidation of the target surface provided enough uranium oxides to produce the UO^- and UO_2^- anions. After passing through a skimmer, anions from the cluster beam were extracted perpendicularly into a modified Wiley-McLaren time-of-flight mass spectrometer. Species of interest were then mass selected before entering the interaction zone of the imaging lens. A tunable Continuum Sunlite EX OPO, pumped with an injection-seeded Continuum Powerlite laser, was used for photodetachment. Photon energies for the current experiment were between 1.1696 and 2.5005 eV with ~150 μJ per pulse and a line width <0.3 cm^{-1}. The detachment laser was calibrated over a range of photon energies using a Bristol 821 series pulsed wavelength meter. The difference between the measured and expected photon energies was typically around 0.1 meV (~0.8 cm^{-1}).

Photoelectrons were focused onto a micro-channel plate coupled to a phosphorus screen and a charge-coupled device (CCD) camera. The repeller voltage of the imaging lens was −300 V for spectra taken at photon energies below 1.5001 eV and −800 V for the spectrum measured at 2.5005 eV photon energy. A half-wave plate and a Glan-laser polarizer were used to ensure the polarization of the detachment laser was parallel to the imaging detector. The recorded 2-dimensional (2D) images were converted to 3D using an inverse-Abel transformation in the BASEX program.[32] Typical experiments required 100 000–200 000 laser shots with the exception of the 2.5005 eV spectrum, which required about 500 000 shots to obtain satisfactory signal-to-noise ratios. The resolution of the current imaging lens can reach 1-3 cm^{-1} for low energy electrons, as described previously.[28–31]

An important piece of information obtained in photoelectron imaging is the anisotropy parameter (β), which describes the angular distributions of photoelectrons. This can be calculated from the reconstructed images by analyzing the photoelectron differential cross-sections (σ),[33]

$$d\sigma/d\Omega = \sigma_{total}/4\pi[1 + \beta P_2(\cos\theta)], \quad (1)$$

where $P_2(\cos\theta) = \frac{1}{2}(3\cos^2\theta - 1)$ is the second order Legendre polynomial, and θ is the angle of the ejected electron relative to the polarization of the laser. The photoelectron angular distribution (PAD) is given by

$$dI(\theta) \sim [1 + \beta P_2(\cos\theta)], \quad (2)$$

where β is the anisotropy parameter, which has values between $-1 \le \beta \le 2$. This model works well for particles that are ejected from randomly oriented molecules undergoing an electronic transition if only a single photon is absorbed. For detachment from pure atomic orbitals with angular momentum l, the ejected photoelectrons will carry angular momentum, $l \pm 1$. For detachment from a pure atomic s-orbital, hence, the outgoing wave will have $l = 1$ (pure p-wave) and $\beta = 2$. The value of β for molecular orbitals is more difficult to interpret because they are linear combinations of atomic orbitals. It has been determined that photoelectrons originating from a σ orbital will converge to a β value between 1.5 and 2.0.[34] Detachment from a π orbital will converge to a value for $\beta < 0$ and detachment from a δ orbital will converge to a value for $\beta > 0$.[34] Only peaks observed at multiple photon energies with high intensity will yield values for β in this study. Spectral transitions with low signal-to-noise ratios did not allow us to accurately fit Eqs. (1) and (2).

III. EXPERIMENTAL RESULTS

A. UO_2^-

Figure 1 shows the photoelectron spectrum taken at a photon energy of 2.5005 eV. Several intense peaks (X, A, a, and B) are observed in the low binding energy range with numerous weak peaks (b-g) beyond 1.6 eV. Vibrational progressions for the X, A, and B states are labeled. This spectrum is similar to the 532 nm spectrum reported recently using our magnetic-bottle PES apparatus,[20] but better resolved with the current imaging apparatus. The labels for the low binding energy peaks are similar to the previous report, but the weak peaks are labeled differently because some of the weak peaks are not observed in the current spectrum due to the poorer signal-to-noise ratios or the photon-energy dependent intensity change.

Higher resolution spectra are measured for the low binding energy part of the spectrum at lower photon energies: 1.1796, 1.2297, 1.3299, and 1.5001 eV, as shown in Fig. 2. The peak

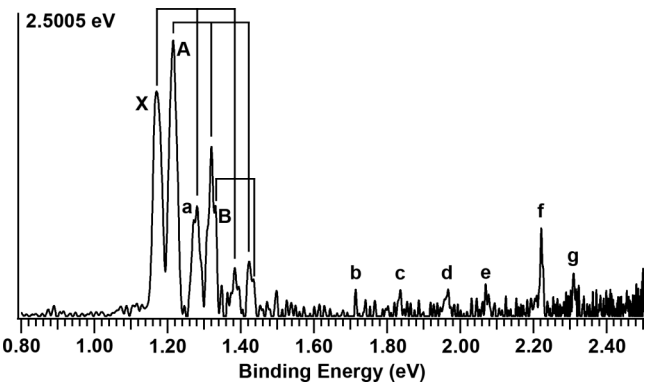

FIG. 1. The photoelectron spectrum of UO_2^- at 2.5005 eV. The vertical lines represent the vibrational progressions for the ground state (X), first excited state (A), and the second excited state (B).

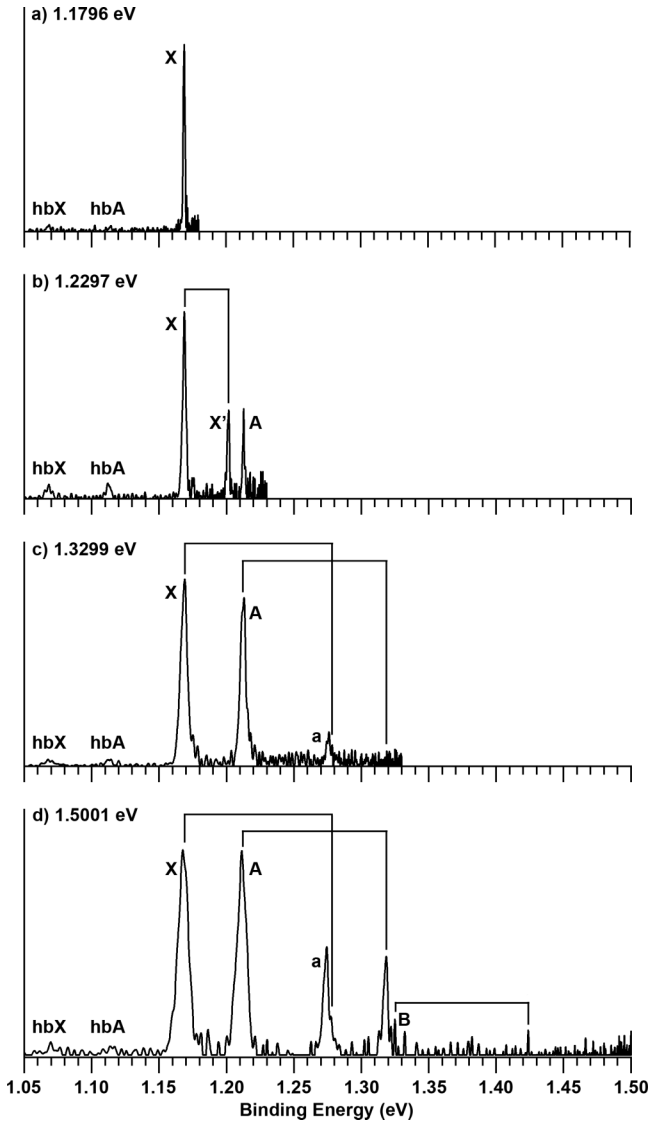

FIG. 2. High resolution photoelectron spectra of UO_2^- at photon energies between 1.1796 and 1.5001 eV. The vertical lines represent vibrational progressions of the ground state (X), first excited state (A), and the second excited state (B).

labeled as X represents the detachment transition from the ground state of the UO_2^- to that of the neutral UO_2 and defines the EA of UO_2 accurately as 1.1688 ± 0.0006 eV, measured from the lowest photon energy spectrum at 1.1796 eV (Fig. 2(a)). A short vibrational progression is observed from this transition with a frequency of about 856 ± 6 cm^{-1} (Figs. 1, 2(c), and 2(d)), corresponding to the symmetric stretching mode of the ground state of UO_2. The peak A at a binding energy 1.2118 ± 0.0006 eV corresponds to the first excited state of UO_2. A vibrational progression is also observed with a frequency of 840 ± 12 cm^{-1} (Fig. 2(d)). A second excited state, B, with much weaker intensity (Fig. 2(d)) is discerned as the shoulder of the first vibrational peak of peak A with a binding energy of 1.3244 ± 0.0006 eV. The B state exhibits a vibrational progression with a frequency of 796 ± 3 cm^{-1}. This transition has higher intensity at higher detachment photon energies, as shown in Fig. 1, as well as at 532 nm previously.[20]

The spectrum at 1.2297 eV (Fig. 2(b)) clearly shows a peak labeled as X′ at 1.2003 ± 0.0007. This peak is assigned as the bending mode of the ground state, for which symmetry selection rules allow only for the observation of levels with even quanta. This assignment provides a vibrational spacing for the even quanta of 254 ± 7 cm^{-1} or a bending frequency of $\nu_2 = 127 \pm 7$ cm^{-1}, which is in good agreement with the previous experimental value.[16] Surprisingly, the bending mode is not observed in the 1.3299 eV spectrum (Fig. 2(c)) and the 1.5001 eV spectrum (Fig. 2(d)). In our previous study, at 532 nm, the bending mode was observed for the A state, but it is not observed in the current spectra (Figs. 1, 2(c), and 2(d)). This photon energy dependence of the bending excitation is interesting and is not currently understood.

Two hot bands are also observed clearly in Figure 2. The peak at 1.0654 ± 0.0013 eV (hbX) is assigned as the transition from the vibrational hot band of the symmetric stretching mode of the anion to the ground state vibrational and electronic state of neutral UO_2. A stretching frequency of 830 ± 10 cm^{-1} is measured for the UO_2^- anion. The peak labeled hbA is assigned to the transition from the hot band of the stretching mode of the anion ground state to the vibrational ground state of the first excited state (A) of UO_2. A frequency is measured to be 820 ± 10 cm^{-1}. Taking the average of the two hot band transitions, we estimate a stretching frequency of 825 ± 10 cm^{-1} for the UO_2^- anion.

Table I lists the adiabatic detachment energies (ADEs) of all the observed detachment transitions of UO_2^-. It should be noted that peaks X and A were derived from a single electron detachment with the removal of an electron from the $2\sigma_g$ (7s) orbital and peaks a, B, and C were derived from two-electron transitions.[20] The remaining peaks (b-g) were assigned qualitatively due to the high density of states and will be discussed below.[20] Table II summarizes the vibrational frequencies of UO_2^- and the three low-lying electronic states of UO_2. The binding energies of all these peaks are given in Table I and compared with those reported in Ref. 20.

Finally, we are able to obtain the β values for the ground state transition (X), the bending mode (X′), and the first excited state (A). These values are plotted with respect to the electron kinetic energy in Figure 3.

B. UO^-

Fig. 4 presents the PE spectra of UO^-, revealing a number of well-resolved detachment transitions. The peak labeled X corresponds to the detachment transition from the ground state of UO^- to that of neutral UO and defines the EA of UO accurately as 1.1407 ± 0.0007 eV from the 1.1696 eV photon energy spectrum (Fig. 4(a)). A vibrational feature is also observed for the ground state transition (Figs. 4(b) and 4(c)), resulting in a U-O vibrational frequency of 878 ± 8 cm^{-1}, in good agreement with those reported previously.[21] Three relatively weak peaks (A, B, C) are observed just above the ground state at ADEs of 1.1524 ± 0.0008, 1.1586 ± 0.0005, and 1.1748 ± 0.0016 eV, respectively. A strong peak D is observed at 1.2699 ± 0.0006 eV, which has a vibrational feature with a stretching frequency of 849 ± 6 cm^{-1}. Table III summarizes the ADEs of all the observed detachment transitions, while Table IV lists the observed vibrational frequencies compared to previous works. We have also determined the β values for

TABLE I. Summary of all observed electronic states of UO_2 compared with the previous experimental and theoretical values. The leading configurations are shown in bold face. Uncertainty of the last digit(s) is given in parentheses.

	Current Experiment		Previously Reported Values[a]			
Peak	ADE (eV)	ΔE (cm^{-1})	VDE (eV)	Calc. (eV)	Ω	Composition of SR states
X	1.1688 (6)	0	1.159 (20)	1.159	2_u	89% $^3\Phi_u(\mathbf{2\sigma_g 1\phi_u})$ + 8% $^3\Delta_u(2\sigma_g 1\delta_u)$
A	1.2118 (6)	347 (5)	1.202 (20)	1.204	3_u	51% $^3\Phi_u(\mathbf{2\sigma_g 1\phi_u})$ + 36% $^1\Phi_u(\mathbf{2\sigma_g 1\phi_u})$ + 13% $^3\Delta_u(2\sigma_g 1\delta_u)$
B	1.3244 (6)	1255 (5)	1.339 (20)	1.367	1_u	98% $^3\Delta_u(\mathbf{2\sigma_g 1\delta_u})$
C	...	...	1.384 (30)	1.417	2_u	56% $^3\Delta_u(\mathbf{2\sigma_g 1\delta_u})$ + 41% $^1\Delta_u(\mathbf{2\sigma_g 1\delta_u})$
a	1.2758 (11)	863 (9)	1.282 (30)	1.283	4_g	93% $^3H_g(\mathbf{1\phi_u 1\delta_u})$
b	1.7144 (12)	4401 (10)	1.74 (4)	1.741	1_g	48% $^3\Pi_g(\mathbf{1\phi_u 1\delta_u})$ + 35% $^3\Sigma_g^-(1\delta_u^2 + \mathbf{1\phi_u^2})$ + 13% $^1\Pi_g(\mathbf{1\phi_u 1\delta_u})$
				1.797	5_g	99% $^3H_g(\mathbf{1\phi_u 1\delta_u})$
				1.799	4_u	100% $^3\Phi_u(\mathbf{2\sigma_g 1\phi_u})$
c	1.8352 (20)	5375 (16)	1.85 (3)	1.840	3_u	47% $^3\Phi_u(\mathbf{2\sigma_g 1\phi_u})$ + 29% $^3\Delta_u(2\sigma_g 1\delta_u)$ + 24% $^1\Phi_u(\mathbf{2\sigma_g 1\phi_u})$
				1.878	3_u	57% $^3\Delta_u(\mathbf{2\sigma_g 1\delta_u})$ + 40% $^1\Phi_u(2\sigma_g 1\phi_u)$ + 2% $^3\Phi_u(2\sigma_g 1\phi_u)$
				1.881	4_u	92% $^3H_u(\mathbf{1\phi_u 1\delta_u})$
d	1.9641 (35)	6414 (28)	1.98 (4)	1.916	2_u	55% $^1\Delta_u(\mathbf{2\sigma_g 1\delta_u})$ + 35% $^3\Delta_u(\mathbf{2\sigma_g 1\delta_u})$ + 10% $^3\Phi_u(2\sigma_g 1\phi_u)$
				2.013	0_u	67% $^1\Sigma_u^-(\mathbf{1\delta_u 1\delta_g})$ + 31% $^3\Sigma_u^+(\mathbf{1\delta_u 1\delta_g})$
e	2.0723 (32)	7287 (26)	2.10 (3)	2.116	3_u	98% $^3\Gamma_u(\mathbf{1\delta_u 1\delta_g})$
				2.167	1_g	61% $^3\Sigma_g^-(\mathbf{1\phi_u^2} + 1\delta_u^2)$ + 21% $^1\Pi_g(\mathbf{1\phi_u 1\delta_u})$ + 15% $^3\Pi_g(\mathbf{1\phi_u 1\delta_u})$
f	2.2223 (21)	8497 (17)	2.22 (4)	2.175	0_g	100% $^3\Pi_g(\mathbf{1\phi_u 1\delta_u})$
				2.214	6_g	95% $^3H_g(\mathbf{1\phi_u 1\delta_u})$
				2.257	5_u	85% $^3H_u(\mathbf{1\phi_u 1\delta_g})$ + 12% $^3\Gamma_u(1\delta_u 1\delta_g)$
g	2.3105 (21)	9208 (17)	2.31 (3)	2.263	2_g	93% $^3\Pi_g(\mathbf{1\phi_u 1\delta_u})$
				2.277	1_u	40% $^3\Pi_u(\mathbf{1\phi_u 1\delta_g})$ + 28% $^3\Sigma_u^+(1\delta_u 1\delta_g)$ + 28% $^1\Pi_u(\mathbf{1\phi_u 1\delta_g})$
				2.305	0_g	63% $^3\Pi_g(\mathbf{1\phi_u 1\delta_u})$+25% $^1\Sigma_g^+(1\delta_u^2+\mathbf{1\phi_u^2})$
				2.408	0_u	65% $^3\Pi_u(\mathbf{1\phi_u 1\delta_g})$ + 24% $^3\Sigma_u^+(1\delta_u 1\delta_g)$ + 11% $^1\Sigma_u^-(1\delta_u 1\delta_g)$

[a]Ref. 20.

the three more intense peaks in the PE images of UO^-, as shown in Fig. 5 as a function of the electron kinetic energy.

IV. DISCUSSION

A. UO_2^-

The current high-resolution PE imaging data on UO_2^- are consistent with the recently reported PE spectra at 532 nm.[20] Hence, the interpretation will be largely based on the recent work. The ground electronic state of UO_2^- is known to be $^2\Phi_{5/2u}$ ($2\sigma_g^2 1\phi_u^1$).[20] The first excited state of the anion ($^2\Delta_{3/2u}$) is calculated at the SO-CASPT2 level of theory to lie 0.26 eV higher in energy and it is not expected to be populated experimentally.[20] Thus, all the detachment transitions should correspond to the ground state of UO_2^-.[20] The current more accurate EA of 1.1688 ± 0.0006 eV for UO_2 agrees with the previous value of 1.159 ± 0.020 eV.[20] Table I compares the current data with the previous experimental and theoretical data reported in Ref. 20 where all the vertical detachment energies (VDEs) were offset by 0.062 eV for comparison to the experimental data.

No vibrational structures were resolved for the ground state transitions in the previous PE study.[20] In the current work, two vibrational modes are resolved for the ground state: the symmetric stretching mode (856 ± 6 cm^{-1}) and the bending mode ($\nu_2 = 127 \pm 7$ cm^{-1}). The stretching frequency has been calculated in a number of previous studies in the range of 809–896 cm^{-1},[1–3,13] all in fairly good agreement with the current value. The bending frequency observed in the current work is in excellent agreement with a previous experimental report of 120 ± 10 cm^{-1}.[16] The current stretching and bending frequencies observed for the ground electronic state of UO_2 are compared with previous calculations in Table II. The hot band transitions yield a stretching frequency of 825 ± 10 cm^{-1} for the UO_2^- anion, in excellent agreement with two previously calculated values of 832 and 825 cm^{-1}.[1,3]

The peak corresponding to the even quanta of the bending mode (X′ in Fig. 2(b)) has a β value of nearly zero at a kinetic energy of 0.0294 eV (Fig. 3). This β value is quite different from that of the nearby peak A, which has a β value of 1.04 at a kinetic energy of 0.0179 eV (Fig. 3). Despite the fact that both transitions are from detachment from the $2\sigma_g$ orbital, the

TABLE II. Vibrational frequencies of UO_2^- and UO_2 compared with the previously reported experimental and theoretical values. Uncertainty of the last digit(s) is shown in parentheses.

			Current Experiment	Previously Reported Values				
Peak	Ω	Mode	Frequency (cm^{-1})	Expt. (cm^{-1})	Theo. (cm^{-1})			
hbX								
	3_u	σ_g	825 (10)	...	825[a]	832[b]	...	...
hbA								
X	2_u	π_u	127 (7)	120 (10)[c]	138[a]	149[b]	81[d]	...	...
		σ_g	856 (6)	...	874[a]	892[b]	863[d]	856[e]	809[f]
A	3_u	σ_g	840 (12)	870 (50)[g]	883[a]	...	...	...	796[f]
B	1_u	σ_g	796 (3)	810 (50)[g]	...	...	...	...	781[f]

[a]Ref. 1.
[b]Ref. 3.
[c]Ref. 16.
[d]Ref. 8.
[e]Ref. 13.
[f]Ref. 2.
[g]Ref. 20.

difference in β value is probably due to a final state effect. A model has been proposed previously to determine the β parameter of a molecular orbital by using linear combinations of all outgoing waves weighted by the population of each atomic orbital that contributes to the molecular orbitals.[35] This model has shown that transitions from the same molecular orbital to different final states result in different values for β.[35] One limitation of this model is the lack of photon energy dependent effects to the interference term and phase shift from the Cooper-Zare formula.[36] In addition, this model requires quantum chemical calculations that are outside the scope of this report so it will only be used qualitatively. Therefore, we will only use the sign and magnitude of β to extract information about the relative peak intensities, because, according to the Wigner threshold law, intensity will decrease for electrons with angular momentum $l > 0$ near threshold.[37] The smaller β value at low kinetic energies means peak X′ should have a larger cross-section, relative to that of peak A at this photon energy, as observed in Fig. 2(b). The electronic transition for peak X′ is the same as peak X, whose β value rises rapidly with increasing photon energy (Fig. 3), so we expect the value of β for X′ to rise rapidly as well. Hence, the rapid increase of the β value with photon energies could partially explain why the detachment cross section for the X′ peak diminishes in Figs. 2(c) and 2(d). In the meantime, the cross section for peak A increases with photon energies, becoming the most intense peak in the 2.5005 eV photon energy spectrum (Fig. 1).

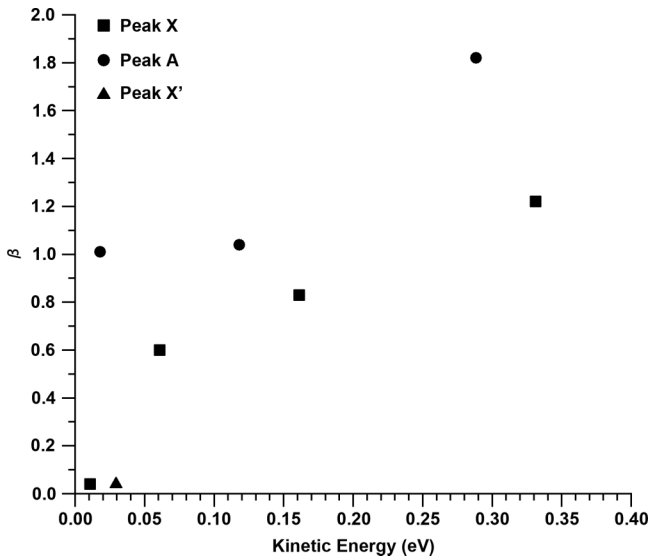

FIG. 3. Anisotropy parameters (β) obtained for UO_2 from peaks X, X′, and A at various electron kinetic energies.

Peak A represents the detachment transition to the first neutral excited state ($^3\Phi_{3u}$) (Table I). The excitation energy of the A state is 347 cm^{-1}, in good agreement with previous experimental and theoretical results.[1,2,4,6,7,15,16,20] The β value for the A state converges to 2, as the electron kinetic energy increases (Fig. 3). This observation is consistent with the assignment that the first excited state results from detachment from the $2\sigma_g$ orbital, which mainly consists of the uranium 7 s orbital (outgoing p-wave with $\beta = 2$). Our observed frequency of 840 ± 12 cm^{-1} for the symmetric stretching mode of the A state agrees well with previous experimental and theoretical values (Table II).[1,2,20] Surprisingly, we did not observe the bending mode for this state that was observed in the previous PES study.[20] We suspect that this is due to the fact that the anisotropy parameter of the outgoing wave is greater than zero, and therefore, the detachment cross section is not favored when the photon energy is just above the threshold.

The next peak, B, corresponds to the second excited state ($^3\Delta_{1u}$) of UO_2 (Table I). The excitation energy of the B state is measured quite accurately to be 1255 ± 5 cm^{-1}, which agrees with the value of 1400 ± 150 cm^{-1} obtained previously using fluorescence spectroscopy in an argon matrix[15] and the previous PES study.[20] The obtained stretching frequency in the current study is 796 ± 3 cm^{-1}, consistent with previous experimental and theoretical values (Table II).[2,20] However, one difference with the previous magnetic-bottle PES experiment is the feature with a binding energy of 1.38 eV in Fig. 1. The previous report tentatively assigned this peak as another excited state [56% $^3\Delta_{2u}(2\sigma_g 1\delta_u) + 41\%\,^1\Delta_{2u}(2\sigma_g 1\delta_u)$] (Table I), due to the fact that it did not fit into a vibrational progression. The current high-resolution data show that it is better to assign

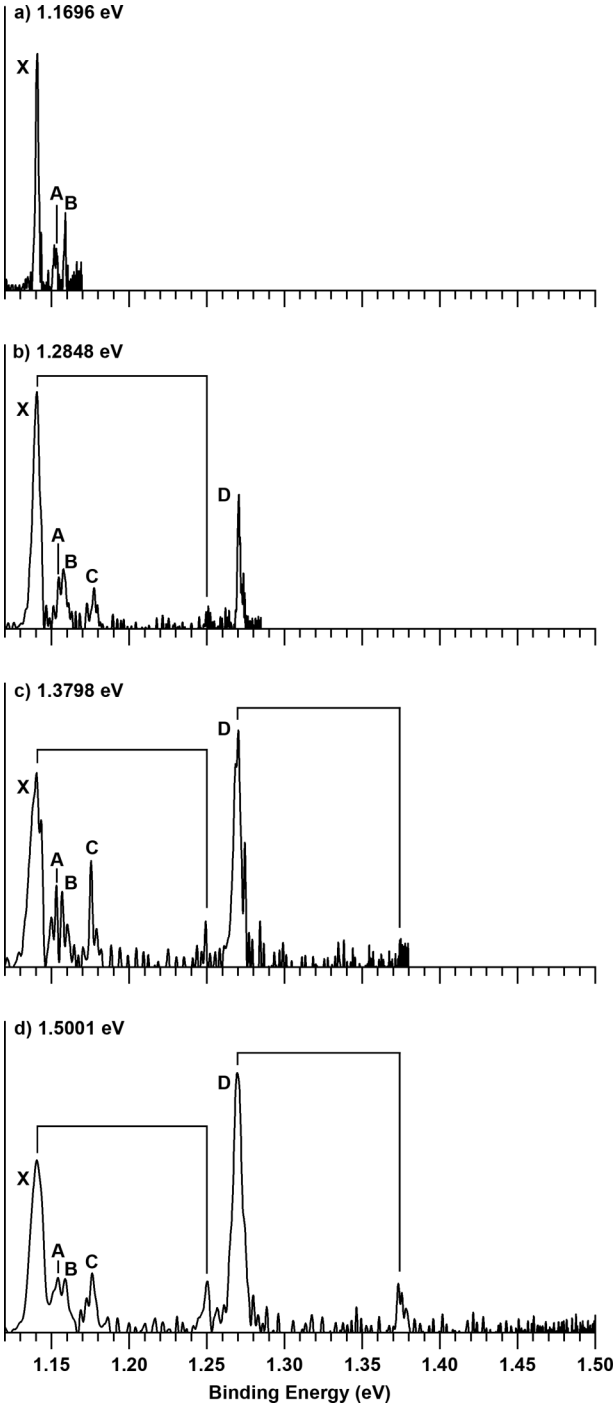

FIG. 4. Photoelectron spectra of UO^- at photon energies between 1.1696 and 1.5001 eV. The vertical lines represent the vibrational progressions of peaks X and D.

it as part of the stretching vibrational progression of the ground state X. It is possible that one of the shoulders on either side of the 1.38 eV peak could correspond to this excited state. Unfortunately, the detachment cross section is too low in the high resolution spectrum at 1.5001 eV (Fig. 2(d)) to allow a more definitive assignment.

The peaks labeled B and a were attributed to two-electron processes previously.[20] Most of the transitions assigned to peaks b–g are also due to two-electron processes, where there is one-electron detachment from one of the $2\sigma_g{}^2 1\phi_u{}^1$ orbitals while another electron is simultaneously excited to a higher-lying unoccupied 5f, 6d, or 7p orbital, with the exception of the $^3\Phi_{4u}$ state under peak b and the $^3\Phi_{3u}$ state under peak c which correspond to one-electron detachment processes.[20] However, it should be noted that peaks b-g were only qualitatively assigned because of the extremely high density of states, the limitation of the accuracy using approximate quantum mechanical and relativistic methods, and the unsaturated atomic basis sets used for such a complicated system as previously reported.[20] Table I compares the current observations with the previous experimental and theoretical data performed using *ab initio* wave function theory with the multi-configurational approach including spin-orbit and relativistic effects in our previous study.[20] The calculated VDEs were in good agreement with the current results. The current data are consistent with the previous experimental results, except one feature at 1.63 eV, which was labeled as "b" in the previous PES study,[20] but it is clearly not observed in the current study at 2.5005 eV (Fig. 1). These multi-electron transitions are due to the strong electron correlation effects and they have very weak detachment cross sections. The difference in the two studies could be a result of photon energy dependent detachment cross sections.

B. UO^-

The electronic structures of the ground state and many excited states of UO have been determined previously.[5,21–24] Low-lying states of UO were reported in a previous experimental study to arise from two configurations: $U^{2+}(5f^37s^1)O^{2-}$ and $U^{2+}(5f^27s^2)O^{2-}$,[23,24] while the ground state of UO was confirmed to have a leading term of $^5I_4$ from the $U^{2+}(5f^37s^1)O^{2-}$ configuration validating the use of ligand field theory in the understanding of the low-lying electronic states of the molecule.[25] To the best of our knowledge, no theoretical studies have been performed on the UO^- anion, so it is not clear what the lowest energy configuration is. Studies in transition metal oxides have shown that the valence s orbital is stabilized as the charge state is changed from MO^+ to MO and then to MO^-.[34,38–40] Similarly, the electronic ground state of UF, isoelectronic to UO^-, was clearly identified as $|\Omega| = 4.5$, confirming the theoretically predicted $U^+(5f^37s^2)F^-$ configuration.[26,27] Thus, one would expect the most likely configuration for UO^- to be $U^+(5f^37s^2)O^{2-}$, $^4I_{4.5}$. Under this assumption, removal of a 7s electron will remove ±0.5 units of spin angular momentum along the axis preferentially forming a molecule with $\Omega = 4$ or 5, which agrees with the strong peaks X and D observed in our PE spectra (Fig. 4 and Table III).

Our PE spectrum at 1.1696 eV (Fig. 4(a)) gives rise to an accurate EA for neutral UO as 1.1407 ± 0.0007 eV, defined by the X band, which represents the detachment transition from the ground state of UO^- to that of UO. We observed a vibrational frequency of 878 ± 8 cm^{-1} for the ground state of UO. This frequency is in good agreement with the gas phase measurements reported from the Heaven group,[22] shown in Table IV.

The separation of peaks X and D is 1042 ± 7 cm^{-1}, in excellent agreement with the excitation energy of 1043.00 ± 0.03 cm^{-1} observed for an excited state of UO previously

TABLE III. ADEs of UO^- compared with the available literature. Uncertainty of the last digit(s) is shown in parentheses.

	Current experiment		Reported values	
Peak	ADE (eV)	ΔE (cm^{-1})	ΔE (cm^{-1})[a]	Orbital population analysis[b]
X	1.1407 (7)	0	0	63% $^5I_4(1\varphi^1 2\delta^1 4\pi^1 6\sigma^1)$ + 14% $^5H_4(1\varphi^1 2\delta^1 7\sigma^1 6\sigma^1)$
A	1.1524 (8)	94 (9)	...	...
B	1.1586 (5)	144 (7)	...	...
C	1.1748 (16)	275 (14)	294.12 (2)	64% $^3H_4(1\varphi^1 2\delta^1 6\sigma^2)$ + 12% $^5I_4(1\varphi^1 2\delta^1 4\pi^1 6\sigma^1)$
D	1.2699 (6)	1042 (7)	1043.00 (3)	37% $^5I_5$ $(1\varphi^1 2\delta^1 4\pi^1 6\sigma^1)$ + 18% $^3I_5$ $(1\varphi^1 2\delta^1 4\pi^1 6\sigma^1)$ + 13% $^5H_5(1\varphi^1 2\delta^1 7\sigma^1 6\sigma^1)$

[a]Ref. 22.
[b]Ref. 5.

by the Heaven group.[22] This excited state was calculated to have the $U^{2+}(5f^3 7s^1)O^{2-}$ configuration with $\Omega = 5$ and a leading term of $^5I_5(1\phi^1 2\delta^1 4\pi^1 6\sigma^1)$.[5] The vibrational frequency we observed for this excited state (849 ± 6 cm^{-1}) also agrees well with the previously reported value of 841.6 ± 1.4 cm^{-1}.[22,23] The assignment of this excited state suggests that the ground state of UO^- should have a configuration of $U^+(5f^3 7s^2)O^{2-}$.

Peaks A, B, and C all have relatively low intensities compared to peaks X and D. The excitation energy of peak C at 275 ± 14 cm^{-1} (Table III) is close to an excited state previously reported at 294.12 cm^{-1} above the ground state.[21–24] This excited state was found to have a total angular momentum value of 4 and was assigned as a state with a leading term of $^3H_4(1\varphi^1 2\delta^1 6\sigma^2)$.[5] This was found to be the lowest energy excited electronic state, which means that peaks A and B might come from detachment transitions from a small population of electronically excited UO^- molecules to the excited states of neutral UO.[5,21–24] It is likely that these excited anions have the $U^+(5f^3 7s^2)O^{2-}$ configuration but with different orbital angular momenta arising from the $5f^3$ configuration. In order to define these transitions, more accurate calculations on the excited states of UO^- are needed.

The β value of the X band increases with kinetic energy and it approaches a value of 1.3, suggesting a *p*-wave detachment channel. It will likely rise above 1.5 with higher kinetic energy. This observation is consistent with detachment of a σ_g electron from UO^-, supporting the possible ground state configuration of $U^+(5f^3 7s^2)O^{2-}$. Similarly, the β value for peak D is about 1.45 at a kinetic energy of 0.23 eV, which is also consistent with detachment from a σ_g orbital as predicted above. Peak C does not converge to a value in the kinetic energies studied, but we suspect it will eventually converge to a value less than zero because it is gradually decreasing. This would be consistent with the predicted detachment from a π orbital.

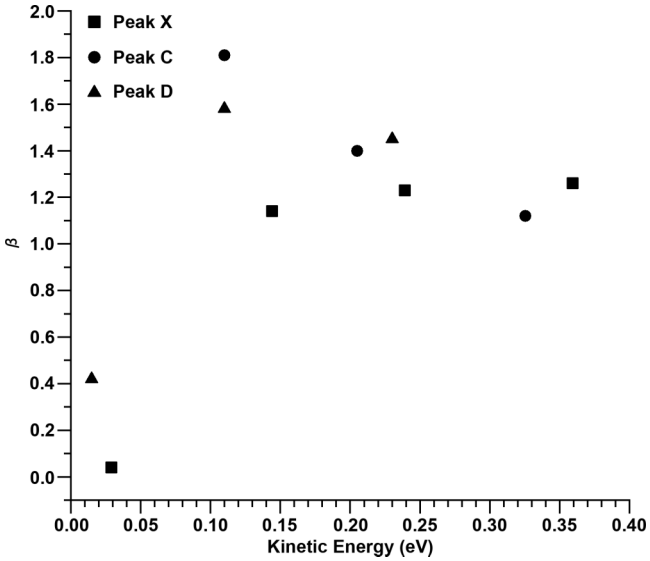

FIG. 5. Anisotropy parameters (β) obtained for UO from peaks X, C, and D at various electron kinetic energies.

TABLE IV. Vibrational frequencies for the ground and excited state of UO compared with available experimental and theoretical works. Values in parentheses represent uncertainty of the last digit(s).

	Current experiment	Reported values	
Peak	Frequency (cm^{-1})	Experimental (cm^{-1})	Theoretical (cm^{-1})[a]
X	878 (8)	820.0 (1),[b,c] 819.3 (1),[d,c] 819.8 (1),[b,e] 889.5 (5),[h,f] 882.35 (60)[i]	846,[f] 869.12[g]
D	849 (6)	841.6 (1.4)[i]	–

[a]Values are unperturbed and not directly comparable to experimental values. See text for explanation.
[b]Obtained in an argon matrix.
[c]Ref. 10.
[d]Obtained in a krypton matrix.
[e]Ref. 12.
[f]Ref. 1.
[g]Ref. 8.
[h]Obtained in a neon matrix.
[i]Ref. 22.

V. CONCLUSIONS

High resolution photoelectron spectra of the UO^- and UO_2^- anions have been obtained using PE imaging. Accurate electron affinities of 1.1688 ± 0.0006 and 1.1407 ± 0.0007 eV have been determined for UO_2 and UO, respectively. Both low-lying electronic structure information and vibrational information have been obtained for UO and UO_2. In addition, the U-O stretching frequency for UO_2^- is observed from the hot band transitions. The electronic and vibrational information for UO_2 and UO are interpreted using previous experimental and theoretical results. Three observed low-lying excited states of UO are assigned by comparing with previous experimental data. The current study provides accurate electronic and vibrational information, which will be valuable to verify further theoretical development.

ACKNOWLEDGMENTS

This material is based on work supported by the U.S. Department of Energy, Office of Basic Energy Sciences, under Award No. DE-SC0006979. The authors are indebted to Professor Michael C. Heaven for valuable discussions and comments and to Dr. Iker León for helpful discussions in the analysis of the anisotropy parameters.

[1]M. Zhou, L. Andrews, N. Ismail, and C. Marsden, J. Phys. Chem. A **104**, 5495 (2000).
[2]L. Gagliardi, B. O. Roos, P. Å. Malmqvist, and J. M. Dyke, J. Phys. Chem. A **105**, 10602 (2001).
[3]D. Majumdar, K. Balasubramanian, and H. Nitsche, Chem. Phys. Lett. **361**, 143 (2002).
[4]L. Gagliardi, M. C. Heaven, J. W. Krogh, and B. O. Roos, J. Am. Chem. Soc. **127**, 86 (2005).
[5]R. Tyagi, Ph.D. thesis, Ohio State University, 2005.
[6]T. Fleig, H. J. Jensen, J. Olsen, and L. Visscher, J. Chem. Phys. **124**, 104106 (2006).
[7]I. Infante, E. Eliav, M. J. Vilkas, Y. Ishikawa, U. Kaldor, and L. Visscher, J. Chem. Phys. **127**, 124308 (2007).
[8]P. Li, T. T. Jia, T. Gao, and G. Li, Chin. Phys. B **21**, 043301 (2012).
[9]D. M. Neumark, J. Phys. Chem. A **112**, 13287 (2008).
[10]S. D. Gabelnick, G. T. Reedy, and M. G. Chasanov, J. Chem. Phys. **58**, 4468 (1973).
[11]D. W. Green, G. T. Reedy, and S. D. Gabelnick, J. Chem. Phys. **73**, 4207 (1980).
[12]R. D. Hunt and L. Andrews, J. Chem. Phys. **98**, 3690 (1993).
[13]J. Li, B. E. Bursten, L. Andrews, and C. J. Marsden, J. Am. Chem. Soc. **126**, 3424 (2004).
[14]I. Infante, L. Andrews, X. Wang, and L. Gagliardi, Chem. Eur. J. **16**, 12804 (2010).
[15]C. J. Lue, J. Jin, M. J. Ortiz, J. C. Rienstra-Kiracofe, and M. C. Heaven, J. Am. Chem. Soc. **126**, 1812 (2004).
[16]J. Han, V. Goncharov, L. A. Kaledin, A. V. Komissarov, and M. C. Heaven, J. Chem. Phys. **120**, 5155 (2004).
[17]J. Han, L. A. Kaledin, V. Goncharov, A. V. Komissarov, and M. C. Heaven, J. Am. Chem. Soc. **125**, 7176 (2003).
[18]J. M. Merritt, J. Han, and M. C. Heaven, J. Chem. Phys. **128**, 084304 (2008).
[19]L. R. Morss, N. M. Edelstein, and J. Fuger, *Chemistry of the Actinide and Transactinide Elements* (Springer, Dordrecht, Neatherlands, 2006), Vol. 1.
[20]W. L. Li, J. Su, T. Jian, G. V. Lopez, H. S. Hu, G. J. Cao, J. Li, and L. S. Wang, J. Chem. Phys. **140**, 094306 (2014).
[21]L. A. Kaledin, J. E. McCord, and M. C. Heaven, J. Mol. Spectrosc. **164**, 27 (1994).
[22]L. A. Kaledin and M. C. Heaven, J. Mol. Spectrosc. **185**, 1 (1997).
[23]L. A. Kaledin, A. N. Kulikov, and L. V. Gurvich, Russ. J. Phys. Chem. **63**, 439 (1989).
[24]L. A. Kaledin and A. N. Kulikov, Russ. J. Phys. Chem. **63**, 942 (1989).
[25]M. C. Heaven, V. Goncharov, T. C. Steimle, T. Ma, and C. Linton, J. Chem. Phys. **125**, 204314 (2006).
[26]I. O. Antonov and M. C. Heaven, J. Phys. Chem. A **117**, 9684 (2013).
[27]M. C. Heaven, B. J. Barker, and I. O. Antonov, J. Phys. Chem. A **118**, 10867 (2014).
[28]Z. Yang, I. León, and L. S. Wang, J. Chem. Phys. **139**, 021106 (2013).
[29]I. León, Z. Yang, and L. S. Wang, J. Chem. Phys. **139**, 194306 (2013).
[30]I. León, Z. Yang, and L. S. Wang, J. Chem. Phys. **140**, 084303 (2014).
[31]I. León, Z. Yang, H. T. Liu, and L. S. Wang, Rev. Sci. Instrum. **85**, 083106 (2014).
[32]V. Dribinski, A. Ossadtchi, V. A. Mandelshtam, and H. Reisler, Rev. Sci. Instrum. **73**, 2634 (2002).
[33]C. N. Yang, Phys. Rev. **74**, 764 (1948).
[34]P. G. Wenthold, R. F. Gunion, and W. C. Lineberger, Chem. Phys. Lett. **258**, 101 (1996).
[35]S. J. Peppernick, K. D. D. Gunaratne, and A. W. Castleman, Jr., Proc. Natl. Acad. Sci. U. S. A. **107**, 975 (2010).
[36]J. Cooper and R. N. Zare, J. Chem. Phys. **48**, 942 (1968).
[37]E. P. Wigner, Phys. Rev. **73**, 1002 (1948).
[38]T. Anderson, K. R. Lykke, D. M. Neumark, and W. C. Lineberger, J. Chem. Phys. **86**, 1858 (1987).
[39]R. F. Gunion, S. J. DixonWarren, W. C. Lineberger, and M. D. Morse, J. Chem. Phys. **104**, 1765 (1996).
[40]D. M. Neumark and W. C. Lineberger, J. Phys. Chem. A **113**, 10588 (2009).